

Comparison of Precipitable Water Vapor Measurements Obtained by Microwave Radiometry and Radiosondes at the Southern Great Plains Cloud and Radiation Testbed Site

B.M. Lesht
Argonne National Laboratory
Argonne, Illinois

J.C. Liljegren
Pacific Northwest National Laboratory
Richland, Washington

Introduction

Comparisons between the precipitable water vapor (PWV) estimated by passive microwave radiometers (MWRs) and that obtained by integrating the vertical profile of water vapor density measured by radiosondes [balloon borne sounding system (BBSS)] have generally shown good agreement (Westwater et al. 1989; England et al. 1992; Ferrare et al. 1995; Liljegren 1994). These comparisons, however, have usually been done over rather short time periods and, consequently, within limited ranges of total PWV and with limited numbers of radiosondes. We have been making regular comparisons between MWR and BBSS estimates of PWV at the Southern Great Plains Cloud and Radiation Testbed (SGP/CART) site since late 1992 as part of an ongoing quality measurement experiment (QME). This suite of comparisons spans three annual cycles and a relatively wide range of total PWV amounts. Our findings show that although the agreement for the most part is excellent, differences between the two measurements occur. These differences may be related to the MWR retrieval of PWV and to calibration variations between radiosonde batches.

The Observations and the Quality Measurement Experiment

The radiosonde measures vertical profiles of pressure, temperature, and relative humidity. Both the microwave radiometer and the radiosonde system were installed at the SGP/CART central facility in May 1992. Regular radiosonde flights have been made since July 1992 and the BBSS/MWR QME was begun in September 1992. The QME uses the radiosonde observations of pressure, temperature, and relative humidity to calculate the vertical profile of absolute water vapor density. This profile is then integrated through the flight

to estimate the total column PWV. The MWR senses atmospheric brightness temperature at two frequencies (23.8 GHz and 31.4 GHz). Retrieval of both integrated column PWV and integrated column liquid water path (LWP) is accomplished using a radiative transfer model. Retrieved quantities are sampled every 20 seconds. For comparison with the PWV obtained from the radiosonde, the 20-second samples are averaged over a 40-minute window centered on the radiosonde launch time. The QME output includes the radiosonde- and MWR-estimated PWV along with statistics describing the variability of the MWR measurements during the averaging period.

Results

Monthly statistics obtained from the BBSS/MWR QME results are shown in Table 1. As will be explained below, these results exclude those comparisons involving radiosondes that were manufactured during November 1994. Precipitation events, as determined by the microwave brightness temperatures, also were excluded because of uncertainties associated with the PWV retrievals under these conditions.

Differences between the PWV estimates are obviously affected by the ability of the radiosondes to accurately measure the in situ water vapor density and also by the veracity of the retrieval algorithms used to convert the brightness temperatures measured by the MWR to columnar integrated water vapor. We have found, overall, that the agreement is generally excellent. The reduction in slope from approximately 1.0 to 0.9 after April 1994 is related to changes in the empirical tuning function used to relate the MWR estimates to the radiosondes.

Time series plots (Figure 1) of the differences between the BBSS and MWR estimates of PWV made at the SGP central facility (CF) and boundary facilities (BFs) occasionally showed sudden shifts in which the radiosondes seemed to be

Table 1. Monthly statistics obtained from the BBSS/MWR QME at the SGP/CART Central Facility. Intercept and slope columns refer to the estimated values of the parameters of a linear model relating the BBSS PWV to the MWR PWV.

Month	PWV _{bbss}	PWV _{mwr}	Δ PWV _{bs-mwr}	RMS Δ PWV	N	Intercept	Slope	r ²
Sep 92	2.09±0.92	2.00±0.98	0.09	0.14	4	-0.20	1.05	0.98
Oct 92	2.11±0.73	1.88±0.74	0.23	0.24	10	-0.35	1.06	0.99
Nov 92	1.27±0.75	1.11±0.67	0.16	0.20	14	0.00	0.88	0.98
Dec 92	1.08±0.74	0.97±0.67	0.11	0.14	17	0.01	0.89	1.00
Jan 93	0.99±0.44	0.91±0.38	0.08	0.12	16	0.07	0.84	0.97
Feb 93	1.07±0.40	1.05±0.42	0.02	0.10	13	-0.02	1.00	0.94
Mar 93	1.00±0.36	0.88±0.36	0.12	0.16	25	-0.09	0.96	0.93
Apr 93	1.25±0.50	1.21±0.46	0.04	0.08	23	0.07	0.92	0.99
May 93	2.34±0.60	2.21±0.57	0.13	0.17	16	0.02	0.94	0.96
Jun 93	3.28±0.62	3.13±0.57	0.16	0.22	55	0.18	0.90	0.94
Jul 93	3.80±0.76	3.63±0.64	0.17	0.25	18	0.48	0.83	0.96
Aug 93	3.24±0.37	3.33±0.41	-0.09	0.16	17	-0.09	1.05	0.89
Sep 93	2.34±1.06	2.32±1.08	0.02	0.09	16	-0.07	1.02	0.99
Oct 93	1.49±0.50	1.50±0.53	-0.01	0.12	19	-0.03	1.02	0.95
Nov 93	0.87±0.43	0.81±0.49	0.06	0.11	19	-0.18	1.14	0.98
Dec 93	1.24±0.74	1.08±0.66	0.17	0.18	4	-0.03	0.89	1.00
Jan 94	0.82±0.38	0.88±0.36	-0.06	0.09	54	0.13	0.92	0.97
Feb 94	0.67±0.36	0.79±0.39	-0.11	0.14	67	0.07	1.07	0.97
Mar 94	0.99±0.36	0.86±0.47	-0.02	0.13	6	-0.25	1.27	0.96
Apr 94	1.87±0.83	1.81±0.58	0.06	0.15	19	0.13	0.90	0.98
May 94	1.18	0.95	0.23	--	1	--	--	--
Jun 94	--	--	--	--	--	--	--	--
Jul 94	2.93±0.82	2.99±0.80	-0.05	0.20	72	0.24	0.94	0.94
Aug 94	3.23±0.77	2.94±0.70	0.29	0.37	124	0.11	0.88	0.91
Sep 94	2.82±1.08	2.46±0.92	0.36	0.43	84	0.09	0.84	0.97
Oct 94	1.28±0.41	1.15±0.34	0.13	0.16	32	0.10	0.83	0.97
Nov 94	1.43±0.80	1.34±0.71	0.09	0.18	134	0.08	0.88	0.97
Dec 94	1.11±0.45	1.10±0.41	0.01	0.10	86	0.10	0.90	0.95
Jan 95	0.92±0.34	0.93±0.31	0.00	0.06	62	0.10	0.90	0.97
Feb 95	--	--	--	--	--	--	--	--
Mar 95	1.22±0.44	1.19±0.40	0.03	0.06	37	0.08	0.90	0.99
Apr 95	1.74±0.56	1.61±0.47	0.13	0.17	56	0.14	0.84	0.98
May 95	2.44±0.85	2.20±0.73	0.24	0.29	108	0.12	0.85	0.97
Jun 95	2.99±0.65	2.71±0.57	0.27	0.31	90	0.18	0.85	0.96
Jul 95	3.38±0.60	3.17±0.56	0.21	0.25	96	0.11	0.91	0.95
Aug 95	3.94±0.89	3.68±0.80	0.25	0.30	60	0.18	0.89	0.98
Sep 95	2.41±1.02	2.29±0.95	0.11	0.18	59	0.07	0.93	0.98
Oct 95	1.57±0.57	1.40±0.51	0.17	0.19	191	0.04	0.87	0.99
Nov 95	1.38±0.55	1.24±0.52	0.14	0.16	89	-0.06	0.94	0.98
All	2.07±1.16	1.93±1.07	0.13	0.22	1867	0.05	0.91	0.98

measuring substantially more water vapor than the MWR. Close examination of the QME results showed that the anomalous radiosondes were manufactured during or just before November 1994.

Further investigation by the radiosonde manufacturer confirmed that the November 1994 radiosondes were calibrated

incorrectly. This error in calibration resulted from a change in the quality control procedures used to verify the performance of the sensors at high relative humidity. As a result, the error in the calibration is greatest at high relative humidity. This may be seen in a scatter plot (Figure 2) showing the QME results at the CF made between July 1, 1995, and September 30, 1995.

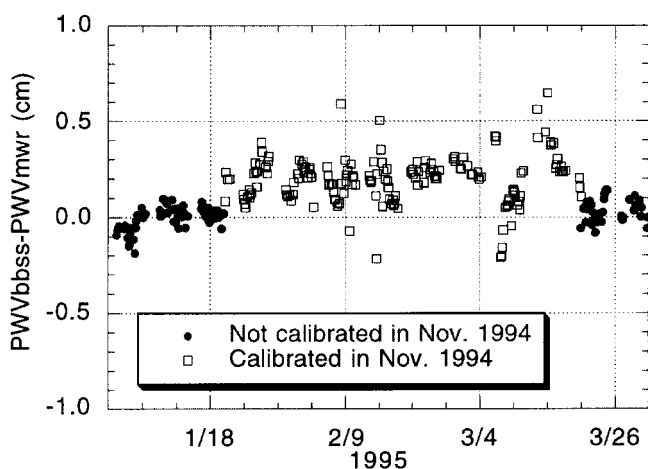


Figure 1. Time series of BBSS/MWR QME results for SGP CF. Closed circles are comparisons using radiosondes not calibrated in November 1994. Open squares are radiosondes calibrated in November 1994.

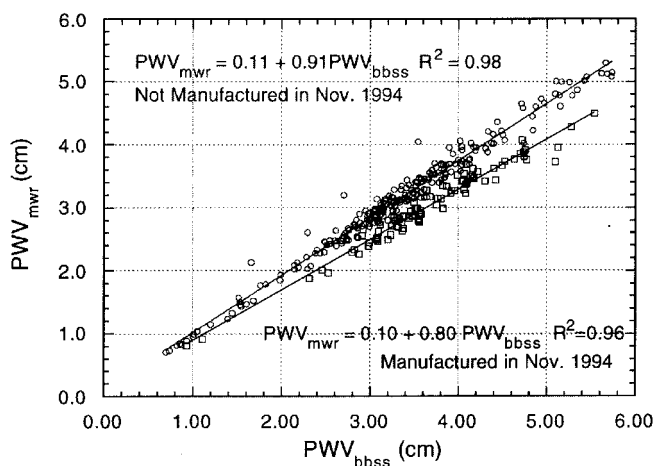


Figure 2. Results of the BBSS/MWR QME for the SGP/CART central facility from 7/1/95 to 9/30/95. Circles are comparisons involving radiosondes not calibrated in November 1994. Squares are comparisons involving radiosondes calibrated in November 1994.

Approximately 1900 incorrectly calibrated radiosondes were used by the Atmospheric Radiation Measurement (ARM) Program. Of these, 1178 were included in the QME results. The distribution of these 1178 radiosondes is shown in Table 2.

Users of CART radiosonde data have been alerted to this problem by publication of a data quality report (DQR).

Table 2. Distribution of incorrectly calibrated radiosondes.

Facility	Number	First Used	Last Used
CF	316	1/20/95	9/22/95
B1	143	2/21/95	9/29/95
B4	313	4/6/95	11/7/95
B5	153	4/14/95	12/14/95
B6	253	3/22/95	10/19/95

Radiosondes from this group can be identified by decoding the radiosonde serial number, which includes the date of calibration. The serial number is included as metadata in the ARM netCDF files in the radiosonde data platforms. For the group of sondes in question, the serial number is of the form DDMMYTTTPP, in which

DD = Day of the month. Note that a leading zero is missing from the netCDF files

MM = Month number + 80 (from 90 to 91 for October and November)

Y = Last digit of the year (4 for 1994)

TT = Calibration batch number on the date of calibration

PP = Position of the sensor package within the calibration tray (0-15)

Thus, the incorrectly calibrated radiosondes have serial numbers coded between 26904TTPP and 22914TTPP.

Discovery of this calibration error in a system as usually reliable as the BBSS highlights one of the subtle benefits of the innovative CART measurement approach. Only by making a large number of measurements under a wide range of conditions was a sufficient amount of data collected to identify the problem. It is quite likely that such an error would not have been found in a typical comparison experiment lasting only a few weeks and using radiosondes from only one calibration batch.

References

England, M.N., R.A. Ferrare, S.H. Melfi, D.N. Whiteman, and T.A. Clark, 1992: Atmospheric water vapor measurements: Comparison of microwave radiometry and lidar. *J. Geophys. Res.* **97**(D1):899-916.

Ferrare, R.A., S.H. Melfi, D.N. Whiteman, K.D. Evans, F.J. Schmidlin, and D.O'C. Starr, 1995: A comparison of water vapor measurements made by Raman lidar and radiosondes. *J. Atmos. Oceanic Technol.* **12**:1177-1195.

Liljegren, J.C., 1994: Two-channel microwave radiometer for observations of total column precipitable water vapor and cloud liquid water path. *Proceedings of the Fifth Symposium on Global Change, January 23-28, 1994, Nashville, TN*, pp. 262-269. American Meteorological Society, Boston, Massachusetts.

Westwater, E.R., M.J. Falls, and I.A. Popa Fotino, 1989: Ground-based microwave radiometric observations of precipitable water vapor: A comparison of ground truth from two radiosonde observing systems. *J. Atmos. Oceanic Technol.* **6**:724-730.